Mineralogical Magazine (2023), **87**, 887–895
doi:10.1180/mgm.2023.62

CAMBRIDGE UNIVERSITY PRESS

Article

Ferriandrosite-(Ce), a new member of the epidote supergroup from Betliar, Slovakia

Martin Števko[1,2], Pavol Myšľan[1,3], Cristian Biagioni[4,5], Daniela Mauro[4] and Tomáš Mikuš[6]

[1]Earth Science Institute v.v.i., Slovak Academy of Sciences, Dúbravská cesta 9, P.O. BOX 106, 840 05 Bratislava, Slovakia; [2]Department of Mineralogy and Petrology, National Museum, Cirkusová 1740, 193 00 Prague 9 – Horní Počernice, Czech Republic; [3]Department of Mineralogy, Petrology and Economic Geology, Faculty of Natural Sciences, Comenius University, Ilkovičova 6, 842 15, Bratislava, Slovakia; [4]Dipartimento di Scienze della Terra, Università di Pisa, Via Santa Maria, 53, I-56126 Pisa, Italy; [5]Centro per l'Integrazione della Strumentazione Scientifica dell'Università di Pisa, Pisa, Italy; and [6]Earth Science Institute v.v.i., Slovak Academy of Sciences, Ďumbierska 1, 974 11 Banská Bystrica, Slovakia

Abstract

A new member of the epidote supergroup, ferriandrosite-(Ce), ideally $MnCeFe^{3+}AlMn^{2+}(Si_2O_7)(SiO_4)O(OH)$, was found at the Július manganese ore occurrence near Betliar, Rožňava Co., Košice Region, Slovakia. It occurs as subhedral grains and polycrystalline aggregates, up to 0.3 mm in size, enclosed in pyroxmangite. Other associated minerals are spessartine, rhodochrosite, quartz, baryte and pyrosmalite-(Mn). Ferriandrosite-(Ce) is dark brown, with a light brown streak and vitreous lustre. The Mohs hardness is ~6½ to 7 and tenacity is brittle with no observable cleavage or fracture. The calculated density is 4.321 g·cm^{-3}. Ferriandrosite-(Ce) is optically biaxial (+), with weak pleochroism, high surface relief and the mean calculated refractive index is 1.832. The empirical structural formula of ferriandrosite-(Ce), based on 13 anions per formula unit, is $^{A1}(Mn^{2+}_{0.63}Ca_{0.35}Ce_{0.02})_{\Sigma 1.00}{}^{A2}(Ce_{0.53}La_{0.27}Nd_{0.14}Pr_{0.05}REE^{*}{}_{0.01})_{\Sigma 1.00}{}^{M1}(Fe^{3+}_{0.41}Al_{0.12}V^{3+}_{0.01}Mg_{0.40}Ti_{0.05})_{\Sigma 0.99}{}^{M2}Al_{1.00}{}^{M3}(Mn^{2+}_{0.75}Fe^{2+}_{0.22}Mg_{0.03})_{\Sigma 1.00}{}^{T1-3}Si_{3.00}O_{11}{}^{O4}(O_{0.67}F_{0.33})(OH)$, where REE* are minor rare earth elements. Ferriandrosite-(Ce) is monoclinic, space group $P2_1/m$, a = 8.8483(4) Å, b = 5.7307(3) Å c = 10.0314(5) Å, β = 113.3659(15)°, V = 466.95(4) Å^3 and Z = 2. The crystal structure of ferriandrosite-(Ce) was refined to a final R_1 = 0.0210 for 1910 reflections with $F_o > 4\sigma(F_o)$ and 127 refined parameters. Structural features of ferriandrosite-(Ce) are discussed and compared with other members of the androsite-series.

Keywords: ferriandrosite-(Ce); new mineral; epidote supergroup; allanite group; crystal structure; manganese mineralisation; Betliar; Slovakia

(Received 10 June 2023; accepted 1 August 2023; Accepted Manuscript published online: 7 August 2023; Associate Editor: Daniel Atencio)

Introduction

The epidote supergroup is composed of mixed-anion silicates with the general formula $A_2M_3[T_2O_7][TO_4](O,F)(OH,O)$ (Armbruster *et al.*, 2006). Currently, this supergroup is represented by 33 monoclinic species, divided into the allanite group (17 species), clinozoisite group (11), and dollaseite group (4); åskagenite-(Nd) is an additional member of this supergroup with O dominant over (OH) at the O10 site. Members of the allanite group are phases rich in rare earth elements (REE), with the following valences at key sites: $A1 = M^{2+}$, $A2 = M^{3+}$, $M1 = M^{3+}$, $M2 = M^{3+}$, $M3 = M^{2+}$, $O4 = O^{2-}$, and $O10 = (OH)^-$ (Armbruster *et al.*, 2006).

During examination of the mineral assemblage of the Július manganese ore occurrence, near Betliar, in Slovakia, a new allanite-group mineral was identified, corresponding to the ideal composition $MnCeFe^{3+}AlMn^{2+}(Si_2O_7)(SiO_4)O(OH)$. Such a composition was reported previously by Girtler *et al.* (2013) and Kolitsch *et al.* (2021) from some occurrences of metamorphosed Mn ores in Austria but no formal proposal for its approval was submitted to the Commission on New Minerals, Nomenclature and Classification of the International Mineralogical Association (IMA-CNMNC). On the basis of the Slovak occurrence, this mineral has been named ferriandrosite-(Ce), in accordance with the existing nomenclature scheme for the epidote-supergroup minerals (Armbruster *et al.*, 2006). The root-name 'androsite' was first used by Bonazzi *et al.* (1996) for a REE-rich member from the Andros Island, Greece, having Mn^{2+} as the dominant cation at the *A*1 and *M*3 sites and the *M*1 site occupied by Mn^{3+}; the prefix 'ferri' indicates the dominance of Fe^{3+} at the *M*1 site for the specimen from the Július manganese ore occurrence. The suffix, indicating the dominant cation at the *A*2 site, agrees with the nomenclature for REE mineral species (Bayliss and Levinson, 1988). The new mineral and its name have been approved by the IMA-CNMNC (IMA2023–022, Števko *et al.*, 2023). The approved mineral symbol of ferriandrosite-(Ce) is Fea-Ce. The holotype specimen of ferriandrosite-(Ce) (polished section Be-5) is deposited in the collections of the Department of Mineralogy and Petrology, National Museum in Prague, Cirkusová 1740, 19300 Praha 9, Czech Republic under the catalogue number P1P 2/2023 and the grain used for the single-crystal X-ray diffraction study is kept in the

Corresponding author: Martin Števko; Email: msminerals@gmail.com
Cite this article: Števko M., Myšľan P., Biagioni C., Mauro D. and Mikuš T. (2023) Ferriandrosite-(Ce), a new member of the epidote supergroup from Betliar, Slovakia. *Mineralogical Magazine* **87**, 887–895. https://doi.org/10.1180/mgm.2023.62

collections of the Museo di Storia Naturale of the Università di Pisa, Via Roma 79, Calci (PI), Italy under catalogue number 20063.

Occurrence and physical properties

Occurrence

Ferriandrosite-(Ce) was found at the Július metamorphosed manganese ore occurrence, which is located on the NE slopes of the Turecká hill (953 m a.s.l.), ~1.4 km WSW of the Betliar village, Rožňava Co., Košice Region, Slovak Republic. Samples with ferriandrosite-(Ce) were collected on September 17, 2019, by one of the authors (MS) from the dump of the main exploration adit (48°41'53.3"N, 20°29'20.1"E).

The Július manganese ore occurrence is situated in the Spišsko-gemerské rudohorie Mts. Small bodies and lenses of metamorphosed carbonate–silicate manganese ore mineralisation are known from several localities in the Spišsko-gemerské rudohorie Mts. (e.g. Čučma-Čierna baňa, Smolník-Hekerová, Betliar-Július), and are hosted in Lower Palaeozoic black phyllites and lydites of the Gelnica Group (Gemeric Unit), metamorphosed in greenschist-facies conditions (Kantor, 1954; Bajaník *et al.*, 1983; Faryad, 1994; Grecula *et al.*, 1995; Rojkovič, 2001; Peterec and Ďuďa, 2003). According to Rojkovič (2001), mineral associations composed of Mn carbonates and silicates in the Spišsko-gemerské rudohorie Mts., mainly represented by rhodochrosite, rhodonite, pyroxmangite, spessartine, tephroite and magnetite, were formed during Variscan metamorphism of sedimentary–diagenetic manganese proto-ores. Subsequent metamorphic–hydrothermal veinlets with quartz, calcite and sulfides represent younger mineralisation stages, probably related to the Alpine orogeny. Ore mineralisation at the Július occurrence was explored in a small scale for manganese and iron in the second half of the 19th century (Maderspach, 1875). In contrast with the nearby and very similar Čučma-Čierna baňa or Smolník-Hekerová manganese deposit, the mineralogy of the small Július manganese ore occurrence was never studied in detail. Maderspach (1875) briefly mentioned rhodonite, rhodochrosite, magnetite, pyrite, 'wad' and 'psilomelane' as principal ore minerals. Ferriandrosite-(Ce) was discovered in a large block of rhodochrosite–spessartine–pyroxmangite–magnetite ore, cut by abundant younger veinlets consisting mainly of coarse crystalline pyroxmangite and spessartine, with minor amounts of quartz, rhodochrosite, baryte and pyrosmalite-(Mn). It occurs rarely as aggregates embedded in pyroxmangite–spessartine veinlets together with rhodochrosite, quartz, baryte and pyrosmalite-(Mn). Its origin is probably due to an Alpine metamorphic–hydrothermal event, favouring the remobilisation of Mn and REE in the Július manganese ore deposit.

Physical and optical properties

Ferriandrosite-(Ce) occurs as subhedral grains and polycrystalline aggregates up to 0.3 mm in size (Figs 1, 2), enclosed in pyroxmangite–spessartine matrix. Ferriandrosite-(Ce) is dark brown, with a light-brown streak and vitreous lustre and it is non-fluorescent in shortwave and longwave ultraviolet light. The Mohs hardness is estimated at ~6½ to 7 based on analogy to other members of the allanite group. It is brittle, with no observable cleavage or fracture. A density of 4.321 g·cm^{-3} was calculated using the unit-cell volume refined from the single-crystal X-ray diffraction data and empirical chemical formula.

Figure 1. Dark brown aggregate of ferriandrosite-(Ce) enclosed in pyroxmangite (light pink)–spessartine (light yellow) matrix. Field of view is 2.06 mm. Photo L. Hrdlovič. Holotype material (P1P 2/2023, polished section Be-5).

Ferriandrosite-(Ce) is optically biaxial (+), with weak pleochroism and high surface relief. Other optical properties were not measured because of relatively strong compositional zoning of the studied aggregates and the presence of intimate intergrowths between the two distinct members of the epidote supergroup. In agreement with Armbruster *et al.* (2006), it is recognised that optical data can be ambiguous and have some limitations in identifying some chemically complex minerals like those belonging to the allanite group. The mean refractive index of ferriandrosite-(Ce), obtained from the Gladstone–Dale relationship (Mandarino, 1979, 1981) using ideal end-member formula and calculated density is 1.832.

Chemical composition

Quantitative chemical (wavelength dispersive spectroscopy) analyses of ferriandrosite-(Ce) were carried out using a JEOL-JXA850F electron microprobe (Earth Science Institute, Slovak Academy of Sciences, Banská Bystrica, Slovakia). The following conditions were applied: accelerating voltage 15 kV, probe current 20 nA, counting time 20s on peak and 10s for background. The diameter of the electron beam ranged from 2–4 μm; ZAF correction was used. The following standards, X-ray lines and crystals were used: diopside (Ca*K*α, PETL and Mg*K*α, TAP); UO_2 (U*M*β, PETL); orthoclase (K*K*α, PETL and Si*K*α, TAP); thorianite (Th*M*α, PETL); tugtupite (Cl*K*α, PETL); crocoite (Pb*M*β, PETL); YPO_4 (Y*L*α, PETL); fluorite (F*K*α, LDE1); albite (Na*K*α, TAP and Al*K*α, TAP); $LaPO_4$ (La*L*α, LIFH); $CePO_4$ (Ce*L*α, LIFH); $NdPO_4$ (Nd*L*α, LIFH); $PrPO_4$ (Pr*L*β, LIFH); $EuPO_4$ (Eu*L*α, LIFH); $SmPO_4$ (Sm*L*β, LIFH); $TbPO_4$ (Tb*L*α, LIFH); $GdPO_4$ (Gd*L*β, LIFH); $ErPO_4$ (Er*L*α, LIFH); $TmPO_4$ (Tm*L*α, LIFH); $DyPO_4$ (Dy*L*β, LIFH); $YbPO_4$ (Yb*L*α, LIFH); $HoPO_4$ (Ho*L*β, LIFH); $LuPO_4$ (Lu*L*α, LIFH); hematite (Fe*K*α, LIF); rhodonite (Mn*K*α, LIF); Cr_2O_3 (Cr*K*α, LIF); $ScVO_4$ (V*K*α, LIF); and rutile (Ti*K*α, LIF). The detection limit (1σ) of every element ranged from 61–881 ppm. REE interferences were solved by overlap corrections as well as F / Fe and F / Ce X-ray line coincidences.

As shown by back-scattered electron images (Fig. 3), the sample studied is chemically zoned. Four different chemical domains were identified. One of them corresponds to the chemical domain

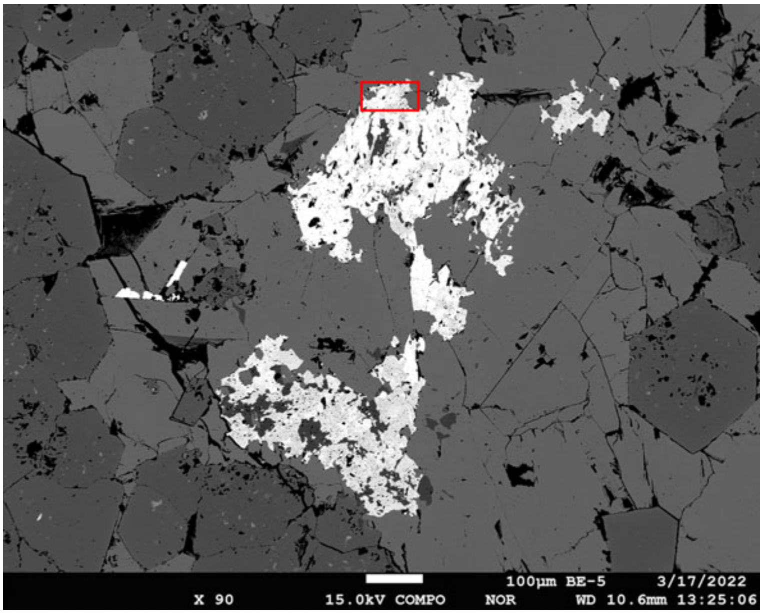

Figure 2. Aggregates and subhedral grains of ferriandrosite-(Ce) (white) enclosed in pyroxmangite (light grey) associated with euhedral crystals of spessartine (dark grey). The red box indicates the area where the grain used for single-crystal X-ray diffraction was picked up. Back-scattered electron (BSE) photo T. Mikuš. Holotype material (P1P 2/2023, polished section Be-5).

('domain A') characterised through single-crystal X-ray diffraction and its chemical data are given in Table 1 (average of 4 spot analyses). The content of Fe_2O_3 and FeO and the amount of H_2O were recalculated in order to achieve 8 (A+M+T) atoms per formula unit (pfu). If the full oxidation of Fe is not sufficient, then Mn is also partially oxidised.

The empirical formula of ferriandrosite-(Ce), based on 13 anions pfu, distributing the chemical constituents among different structural sites, in agreement with the crystal structure refinement (see below), is (with rounding errors and REE* corresponding to minor REE) $^{A1}(Mn^{2+}_{0.63}Ca_{0.35}Ce_{0.02})_{\Sigma 1.00}$ $^{A2}(Ce_{0.53}La_{0.27}Nd_{0.14}Pr_{0.05}REE^{*}_{0.01})_{\Sigma 1.00}$ $^{M1}(Fe^{3+}_{0.41}Al_{0.12}V^{3+}_{0.01}Mg_{0.40}Ti_{0.05})_{\Sigma 0.99}$ $^{M2}Al_{1.00}$ $^{M3}(Mn^{2+}_{0.75}Fe^{2+}_{0.22}Mg_{0.03})_{\Sigma 1.00}$ $^{T1-3}Si_{3.00}O_{11}$ $^{O4}(O_{0.67}F_{0.33})(OH)$. It corresponds to a ideal formula of ferriandrosite-(Ce) of $MnCeFe^{3+}AlMn^{2+}(Si_2O_7)(SiO_4)O(OH)$.

Table 1 also reports the average compositions of the other three domains (B, C, and D). The crystal chemical formulae for these three domains are the following:

domain B:

$^{A1}(Mn^{2+}_{0.55}Ca_{0.45})_{\Sigma 1.00}$ $^{A2}(Ce_{0.54}La_{0.26}Nd_{0.14}Pr_{0.05}REE^{*}_{0.01})_{\Sigma 1.00}$ $^{M1}(Fe^{3+}_{0.73}Al_{0.02}V^{3+}_{0.01}Mg_{0.10}Fe^{2+}_{0.07}Ti_{0.06})_{\Sigma 0.99}$ $^{M2}Al_{1.00}$ $^{M3}(Mn^{2+}_{0.63}Fe^{2+}_{0.31}Mg_{0.06})_{\Sigma 1.00}$ $^{T1-3}Si_{3.00}O_{11}$ $^{O4}(O_{0.90}F_{0.10})_{\Sigma 1.00}(OH)$;

domain C:

$^{A1}(Mn^{2+}_{0.69}Ca_{0.31})_{\Sigma 1.00}$ $^{A2}(Ce_{0.50}La_{0.24}Nd_{0.16}Pr_{0.05}REE^{*}_{0.01}Ca_{0.04})_{\Sigma 1.00}$ $^{M1}(Fe^{3+}_{0.37}Al_{0.25}Mn^{3+}_{0.13}Mg_{0.24}Ti_{0.01})_{\Sigma 1.00}$ $^{M2}Al_{1.00}$ $^{M3}(Mn^{2+}_{0.82}Mg_{0.18})_{\Sigma 1.00}$ $^{T1-3}(Si_{2.97}Al_{0.03})_{\Sigma 3.00}O_{11}$ $^{O4}(O_{0.70}F_{0.30})_{\Sigma 1.00}(OH)$;

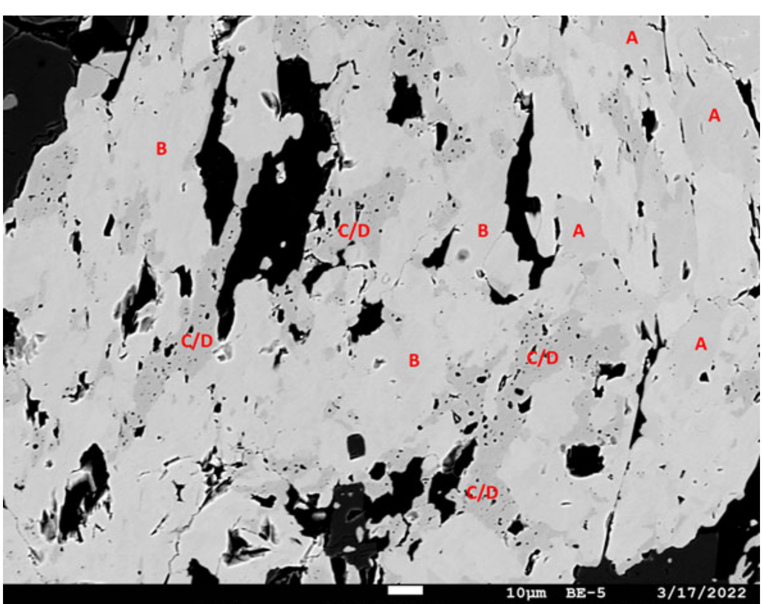

Figure 3. Back-scattered electron (BSE) image showing the chemical inhomogeneity of the material studied. Different chemical domains are shown. Domains C/D are hardly distinguishable in BSE, owing to similar grey hues. BSE photo T. Mikuš.

https://doi.org/10.1180/mgm.2023.62 Published online by Cambridge University Press

Table 1. Electron microprobe data (in wt.%) of ferriandrosite-(Ce) (domains A–C) and associated vielleaureite-(Ce) (domain D).

Domain	A			B	C	D
		Range		wt.%	wt.%	wt.%
Const.	Mean	$n=4$	e.s.d.	$n=8$	$n=2$	$n=2$
SiO_2	29.43	29.29–29.52	0.10	29.02	29.57	29.62
TiO_2	0.67	0.44–0.92	0.21	0.80	0.17	0.17
ThO_2	0.02	0.00–0.04	0.02	0.04	–	–
Al_2O_3	9.29	8.70–9.56	0.40	8.39	10.82	9.05
V_2O_3	0.14	0.09–0.19	0.04	0.18	–	–
Cr_2O_3	0.02	0.00–0.09	0.04	0.01	–	0.06
Y_2O_3	0.01	0.00–0.03	0.01	0.02	0.04	0.04
La_2O_3	7.14	7.04–7.22	0.08	6.92	6.36	7.09
Ce_2O_3	14.86	14.74–14.93	0.08	14.27	13.73	14.58
Pr_2O_3	1.43	1.28–1.60	0.14	1.30	1.39	1.53
Nd_2O_3	3.80	3.62–3.95	0.17	3.85	4.40	4.30
Eu_2O_3	0.14	0.11–0.17	0.03	0.16	0.21	0.13
Dy_2O_3	–	–	–	0.04	–	–
Ho_2O_3	0.05	0.00–0.19	0.10	–	0.04	–
Er_2O_3	0.07	0.00–0.14	0.08	0.07	–	0.03
Tm_2O_3	0.01	0.00–0.05	0.02	0.01	0.04	0.03
Yb_2O_3	–	–	–	0.01	–	–
Lu_2O_3	0.01	0.00–0.05	0.02	–	0.03	0.04
$Fe_2O_{3(tot)}$	8.20	7.84–8.43	0.26	14.23	4.85	2.31
Fe_2O_3 [1]	5.40			9.40		
FeO [1]	2.52			4.35		
MgO	2.84	2.28–3.32	0.43	1.05	2.84	5.46
CaO	3.21	2.91–3.58	0.28	4.03	3.23	1.94
MnO_{tot}	16.00	15.16–17.07	0.80	13.52	19.32	20.67
MnO [1]	16.00			13.52	17.77	17.52
Mn_2O_3 [1]	–	–	–	–	1.73	3.50
PbO	0.01	0.00–0.03	0.01	0.01	–	–
F	1.01	0.86–1.26	0.17	0.32	0.95	1.68
Cl	0.01	0.00–0.01	0.01	0.01	0.02	0.02
H_2O_{calc} [2]	1.47			1.45	1.49	1.50
O = –(F,Cl)	–0.43			–0.14	–0.40	–0.71
Total	99.13			99.06	99.28	99.89

Notes: e.s.d. = estimated standard deviation. The symbol '–' indicates that the chemical constituent was below the detection limit.
[1]Calculated to yield 8 (A+M+T) cations.
[2]Calculated to yield 1 OH group per formula unit.

domain D:

$$^{A1}(Mn^{2+}_{0.78}Ca_{0.21}Ce_{0.01})_{\Sigma1.00}{}^{A2}(Ce_{0.52}La_{0.26}Nd_{0.15}Pr_{0.06}REE^{*}_{0.01})_{\Sigma1.00}$$
$$^{M1}(Mg_{0.51}Mn^{3+}_{0.27}Fe^{3+}_{0.17}Al_{0.03}Ti_{0.01})_{\Sigma1.00}{}^{M2}Al_{1.00}{}^{M3}(Mn^{2+}_{0.70}Mg_{0.30})_{\Sigma1.00}$$
$$^{T1-3}(Si_{2.96}Al_{0.04})_{\Sigma3.00}O_{11}{}^{O4}(F_{0.53}O_{0.47})_{\Sigma1.00}(OH).$$

Domains B and C correspond to the end-member formula $MnCeFe^{3+}AlMn^{2+}(Si_2O_7)(SiO_4)O(OH)$, i.e. to ferriandrosite-(Ce), however domain D leads to end-member formula $MnCeMgAlMn^{2+}(Si_2O_7)(SiO_4)F(OH)$ and corresponds to a recently approved new member of the dollaseite group, vielleaureite-(Ce) (Ragu *et al.*, 2023). The domains A and B can be easily distinguished in back-scattered electron images, whereas C and D domains have similar grey hues. In the material studied, there is a clear positive correlation between Mg and F contents, in agreement with the substitution $^{M1}Fe^{3+} + {}^{O4}O^{2-} = {}^{M1}Mg^{2+} + {}^{O4}F^{-}$ (Fig. 4).

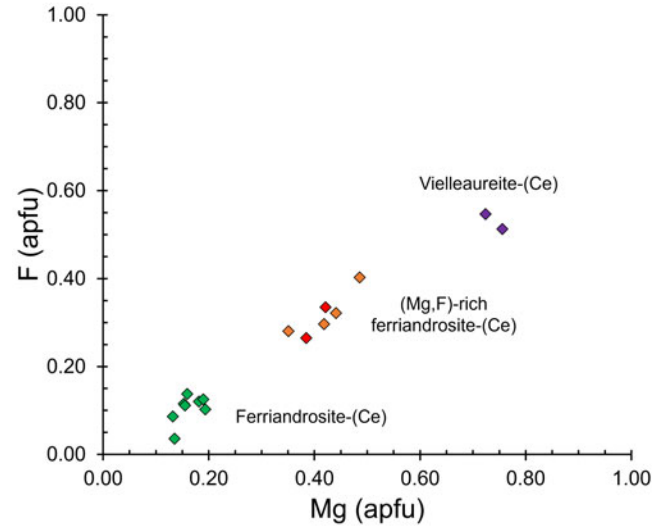

Figure 4. Relationship between F and Mg atoms per formula unit (apfu). Different colours correspond to the chemical homogenous domains: A = orange, B = green, C = red and D = violet.

X-ray crystallography

X-ray diffraction study and structural refinements

Single-crystal X-ray intensity data were collected using a Bruker D8 Venture four-circle diffractometer equipped with an air-cooled Photon III detector, and microfocus Mo*K*α radiation. The detector-to-crystal distance was set to 38 mm. Data were collected using φ scan modes, in 0.5° slices, with an exposure time of 30 s per frame. A total of 1644 frames were collected and they were integrated with the Bruker *SAINT* software package using a narrow-frame algorithm. Data were corrected for Lorentz-polarisation, absorption, and background using the package of software *Apex4* (Bruker AXS, 2022). Unit-cell parameters were refined on the basis of the XYZ centroids of 9895 reflections above 20 σ_I with 7.898° < 2θ < 66.315°. Ferriandrosite-(Ce) is monoclinic, space group $P2_1/m$ (#11), with the following unit-cell parameters: a = 8.8483(4) Å, b = 5.7307(3) Å c = 10.0314(5) Å, β = 113.3659(15)°, V = 10.0314(5) Å^3 and Z = 2.

The crystal structure of ferriandrosite-(Ce) was refined using *Shelxl-2018* (Sheldrick, 2015) starting from the atomic coordinates of ferriakasakaite-(Ce) (Biagioni *et al.*, 2019). The position of the H atoms was located through the difference-Fourier map. The following scattering curves for neutral atoms, taken from the *International Tables for Crystallography* (Wilson, 1992), were used: Mn *vs.* Ca at *A*1, Ce *vs.* Ca at *A*2, Fe *vs.* Mg at *M*1, Al *vs.* Fe at *M*2, Mn *vs.* Mg at *M*3, Si at *T*1–*T*3 sites, H at the H10 site, and O at all the O sites but the O4 position, whose site occupancy was modelled using the scattering curves of O *vs.* F. Refinement of the O/F atomic ratio pointed to $O_{0.65(6)}F_{0.35(5)}$, in agreement with the electron microprobe data. The anisotropic structural model (only H was refined isotropically) converged to R = 0.0210 for 1910 reflections with $F_o > 4\sigma(F_o)$ and 127 refined parameters.

Details of data collection and refinement are given in Table 2. Fractional atom coordinates and equivalent isotropic or isotropic displacement parameters are reported in Table 3. Table 4 reports selected bond distances, whereas Table 5 compares observed and calculated mean atomic numbers at the *A*1, *A*2 and *M*1–*M*3 sites of ferriandrosite-(Ce). Finally, Table 6 gives the weighted bond-valence calculations obtained using the bond-valence parameters of Brese and O'Keeffe (1991). The crystallographic information files have been deposited with the Principal Editor of *Mineralogical Magazine* and are available as Supplementary material (see below).

https://doi.org/10.1180/mgm.2023.62 Published online by Cambridge University Press

Table 2. Crystal and experimental data for ferriandrosite-(Ce).

Crystal data	
Crystal size (mm)	0.115 × 0.055 × 0.040
Cell setting, space group	Monoclinic, $P2_1/m$
a (Å)	8.8483(4)
b (Å)	5.7307(3)
c (Å)	10.0314(5)
β (°)	113.3659(15)
V (Å^3)	466.95(4)
Z	2
Data collection and refinement	
Radiation, wavelength (Å)	Mo*K*α, 0.71073
Temperature (K)	293(2)
$2\theta_{max}$ (°)	66.314
Measured reflections	11900
Unique reflections	1921
Reflections with $F_o > 4\sigma(F_o)$	1910
R_{int}	0.0302
*R*σ	0.0204
Range of *h*, *k*, *l*	$-11 \le h \le 13$
	$-8 \le k \le 8$
	$-15 \le l \le 14$
R [$F_o > 4\sigma(F_o)$]	0.0210
R (all data)	0.0211
wR (on F_o^2)*	0.0533
Goof	1.326
Number of least-squares parameters	127
Maximum and	1.46 (at 1.27 Å from *A*2)
minimum residual peak (e$^-$ Å^{-3})	−0.67 (at 0.75 Å from *A*2)

*$w = 1/[\sigma^2(F_o^2)+(1.6608P)^2]$.

Owing to the inhomogeneous nature of the material studied, powder X-ray diffraction data were collected only on the same crystal used for single-crystal X-ray diffraction, simulating a Gandolfi-like pattern using a Bruker D8 Venture single-crystal diffractometer equipped with a Photon III area detector and microfocused Cu*K*α radiation. The observed X-ray diffraction pattern is reported in Table 7. Unit-cell parameters refined for the monoclinic space group $P2_1/m$ from the powder data using the method of Holland and Redfern (1997) on the basis of 19 unequivocally indexed reflections are as follows: $a = 8.889(2)$ Å, $b = 5.7356(16)$ Å, $c = 10.0262(17)$ Å, β = 113.504(17)°, $V = 468.75(12)$ Å^3 and $Z = 2$.

Table 3. Sites, fractional coordinates and isotropic (*) or equivalent isotropic displacement parameters (in Å^2) for ferriandrosite-(Ce).

Site	*x/a*	*y/b*	*z/c*	U_{eq}/U_{iso}*
*A*1	0.76127(8)	¾	0.15277(6)	0.01271(15)
*A*2	0.59206(2)	¾	0.42861(2)	0.01022(6)
*M*1	0	0	0	0.0093(2)
*M*2	0	0	½	0.0076(3)
*M*3	0.31659(7)	¼	0.20660(6)	0.01323(17)
Si1	0.34794(11)	¾	0.03373(10)	0.00853(18)
Si2	0.69473(11)	¼	0.28300(10)	0.00785(18)
Si3	0.19079(11)	¾	0.32318(10)	0.00731(18)
O1	0.2426(2)	0.9904(3)	0.03055(18)	0.0130(3)
O2	0.3157(2)	0.9723(3)	0.36055(18)	0.0106(3)
O3	0.8047(2)	0.0126(3)	0.33408(19)	0.0123(3)
O4	0.0584(3)	¼	0.1394(3)	0.0130(6)
O5	0.0487(3)	¾	0.1569(3)	0.0115(4)
O6	0.0803(3)	¾	0.4219(3)	0.0099(4)
O7	0.5151(3)	¾	0.1758(3)	0.0139(5)
O8	0.5573(4)	¼	0.3492(3)	0.0190(6)
O9	0.6010(3)	¼	0.1060(3)	0.0140(5)
O10	0.0922(3)	¼	0.4334(3)	0.0100(4)
H10	0.065(9)	¼	0.334(8)	0.041(19)*

Crystal structure description

Ferriandrosite-(Ce) is isotypic with the other members of the epidote supergroup (e.g. Dollase, 1968). The crystal structure can be described as formed by single chains of edge-sharing *M*2-centered octahedra and zig-zag chains of *M*1-centered octahedra with *M*3-centered octahedra attached on alternate sides along *b*. Octahedral chains are bonded to Si_2O_7 and SiO_4 groups. In this octahedral–tetrahedral framework, two kinds of structural cavities occur, i.e. the smaller cavity hosting the nine-fold coordinated *A*1 site and the larger one where the ten-fold coordinated *A*2 site is located.

Cation sites

In ferriandrosite-(Ce), the *A*1 site has a mixed (Mn,Ca) site occupancy, with a Mn/(Mn+Ca) atomic ratio of 0.65. Mean atomic number (Table 5) and weighted bond-valence sum (Table 6) agree with this occupancy. As discussed by previous authors (e.g. Bonazzi *et al.*, 1996; Nagashima *et al.*, 2010, 2013, 2015), the replacement of Ca^{2+} by Mn^{2+} promotes a decrease in the coordination number of the *A*1 site that can be described as six-fold coordinated. This coordination number decrease is related to the shift of the O6 and O9 atoms away from the *A*1 site, whereas O3 and O1 get closer to the cation site; O5 and O7 are unaffected by these changes. If one defines the difference between the bond distances *A*1–O6 and *A*1–O5 (with O6 and O5 being the seventh and sixth ligands of *A*1, respectively) as δ_{7-6}, a direct relation between the Mn^{2+} content at *A*1 and the δ_{7-6} value can be observed (e.g. Bonazzi *et al.*, 1996; Nagashima *et al.*, 2010, 2013, 2015; Biagioni *et al.*, 2019). In ferriandrosite-(Ce), this difference is 0.508 Å, to be compared with the theoretical value of 0.502 Å calculated on the basis of the regression line given by Bonazzi *et al.* (1996). Moreover, a decrease in the $^{[6]}$<*A*1–O> can be observed and indeed, ferriandrosite-(Ce) shows the low value of 2.314 Å, to be compared with 2.320, 2.322, 2.310 and 2.335 Å reported for manganiandrosite-(La), manganiandrosite-(Ce), vanadoandrosite-(Ce) and ferriandrosite-(La), respectively (Bonazzi *et al.*, 1996; Cenki-Tok *et al.*, 2006; Nagashima *et al.*, 2015).

The shift of the O9 site away from the cation located at the *A*1 position is associated with a reduction of the Si1–O9–Si2 bond angle that is related not only to the occupancy at the *A*1 site but also to the average bond length at *M*3 (e.g. Cenki-Tok *et al.*, 2006). In ferriandrosite-(Ce), O9 is at 3.148 and 3.227 Å from *A*1, with a Si1–O9–Si2 bond angle of 137.6(2)°; this angle is similar to those reported by Cenki-Tok *et al.* (2006) for manganiandrosite-(Ce) and vanadoandrosite-(Ce), i.e. 137.4(6) and 137.4(8)°, respectively, and slightly smaller than that given by Nagashima *et al.* (2015) for ferriandrosite-(La), i.e. 139.4(2)°; however, it is smaller than those reported by Biagioni *et al.* (2019) in manganiakasakaite-(La) and ferriakasakaite-(Ce), i.e. 140.88(19) and 144.47(14)°, respectively.

The *A*2 site of ferriandrosite-(Ce) is a REE-bearing site, with Ce as the dominant element. Bonazzi *et al.* (1996) observed a relationship between the ratio of the cell parameters *c*/*V* and the REE content in species belonging to the series piemontite – 'androsite', as well as between the amount of REE and the β angle. In ferriandrosite-(Ce), the *c*/*V* ratio is 0.0215, and the β angle is 113.37°. On the basis of the relationship given by Bonazzi *et al.*

https://doi.org/10.1180/mgm.2023.62 Published online by Cambridge University Press

Table 4. Selected bond distances (in Å) in ferriandrosite-(Ce).

*A*1–O3	2.2463(18) ×2	*A*2–O7	2.351(3)	*M*1–O4	1.9242(16) ×2	*M*2–O3	1.8846(17) ×2
*A*1–O7	2.279(3)	*A*2–O2	2.5104(17) ×2	*M*1–O5	2.0439(18) ×2	*M*2–O10	1.8966(16) ×2
*A*1–O1	2.2911(19) ×2	*A*2–O10	2.580(2)	*M*1–O1	2.0694(18) ×2	*M*2–O6	1.9010(16) ×2
*A*1–O5	2.527(3)	*A*2–O2	2.5969(17) ×2	<*M*1–O>	2.012	<*M*2–O>	1.894
*A*1–O6	3.035(2)	*A*2–O3	2.8710(19) ×2				
*A*1–O9	3.1487(11) ×2	*A*2–O8	2.9572(7) ×2				
*A*1–O9	3.227(3)	<*A*2–O>	2.680				
<*A*1–O>	2.644						
*M*3–O8	2.041(3)	Si1–O7	1.596(3)	Si2–O8	1.600(3)	Si3–O2	1.6301(18) ×2
*M*3–O4	2.110(2)	Si1–O9	1.634(3)	Si2–O3	1.6303(18) ×2	Si3–O5	1.643(3)
*M*3–O2	2.2196(18) ×2	Si1–O1	1.6413(18) ×2	Si2–O9	1.635(3)	Si3–O6	1.644(3)
*M*3–O1	2.2586(19) ×2	<Si1–O>	1.628	<Si2–O>	1.624	<Si3–O>	1.637
<*M*3–O>	2.185						

Table 5. Refined site scattering *vs*. calculated site scattering (in electrons) and site population (in apfu) at the *A* and *M* sites in ferriandrosite-(Ce).

Site	Refined site scattering	Proposed site population	Calculated site scattering
*A*1	23.16	$Mn_{0.65}Ca_{0.35}$	23.25
*A*2	56.29	$Ce_{0.55}La_{0.25}Nd_{0.15}Pr_{0.05}$	58.10
*M*1	18.30	$Fe^{3+}_{0.41}Al_{0.12}V_{0.01}Mg_{0.41}Ti_{0.05}$	18.47
*M*2	13.27	$Al_{1.00}$	13.00
*M*3	24.95	$Mn^{2+}_{0.75}Fe^{2+}_{0.22}Mg_{0.03}$	24.83

(1996), considering ΣREE = 1 atom per formula unit (apfu), one should have $c/V = 0.0213$ and $\beta = 113.4°$, in agreement with observed values. Actually, as stressed by Nagashima *et al.* (2015), the value of the β angle is also affected by the Mn^{2+} at the *A*1 site. The value observed in ferriandrosite-(Ce) can be compared with those reported for other 'androsites', i.e. 113.88° in manganiandrosite-(La) (Bonazzi *et al.*, 1996), 113.84° in ferriandrosite-(La) (Nagashima *et al.*, 2015), 113.42° in manganiandrosite-(Ce), and 113.09° in vanadoandrosite-(Ce) (Cenki-Toc *et al.*, 2006).

Among the three independent *M* sites, cation assignments were based on refined mean atomic numbers (Table 5) and bond-valence sums (Table 6). *M*2 hosts Al only; a possible minor replacement of Al by Fe^{3+} (~2 at.%) or Ti^{4+} (~3 at.%) cannot be discarded, as observed in other samples, e.g. in manganiandrosite-(La) by Bonazzi *et al.* (1996) who reported 4% Fe^{3+} in *M*2 and in ferriandrosite-(La) by Nagashima *et al.* (2015) who hypothesised the presence of 0.04 Ti at the *M*2 site. The <*M*2–O> distance is 1.894 Å, to be compared with those observed in other androsites, i.e. 1.892 Å in manganiandrosite-(La) (Bonazzi *et al.*, 1996), 1.902 and 1.894 Å in manganiandrosite-(Ce) and vanadoandrosite-(Ce), respectively (Cenki-Tok *et al.*, 2006), and 1.902 Å in ferriandrosite-(La) (Nagashima *et al.*, 2015). The *M*3 site is occupied mainly by Mn^{2+}, with minor Fe^{2+} and trace Mg^{2+}. This occupancy is in keeping with the large observed <*M*3–O>, 2.185 Å. This average distance is larger than that observed in manganiandrosite-(La) (i.e. 2.159 Å, where 0.28 M^{3+} apfu occur), and similar to those reported by Cenki-Tok *et al.* (2006) for *M*3 sites in manganiandrosite-(Ce) (2.197 Å) and vanadoandrosite-(Ce) (2.195 Å), where only Mn^{2+} occurs. The slight contraction observed in ferriandrosite-(Ce) is probable due to the minor Fe^{2+}–Mn^{2+} replacement, in agreement with the smaller ionic radius of $^{VI}Fe^{2+}$ (0.78 Å) with respect to that of $^{VI}Mn^{2+}$ (0.83 Å), according to Shannon (1976). The *M*1 site has a complex chemistry, with mainly Fe^{3+} and Mg^{2+}, minor Al and Ti, and trace amounts of V. Whereas Fe^{3+} and Mg^{2+} occur in the same amount (0.41 apfu), the sum of trivalent cations (Fe^{3+} + Al + V) is larger than those of divalent ones (Mg), i.e. 0.54 *vs*. 0.41, with Fe^{3+} as the dominant constituent of the dominant valence (e.g. Bosi *et al.*, 2019a, 2019b). The average bond distance is 2.012 Å, similar to those observed in other androsites, i.e. 2.010, 2.019, 2.011 and 2.002 Å for manganiandrosite-(La), manganiandrosite-(Ce),

Table 6. Weighted bond-valence balance (in vu) in ferriandrosite-(Ce).

	*A*1	*A*2	*M*1	*M*2	*M*3	Si1	Si2	Si3	Σanions
O1	$0.31^{\downarrow\times2}$		$0.39^{\downarrow\times2}$		$0.27^{\downarrow\times2}$	$0.95^{\downarrow\times2}$			1.92
O2		$0.38^{\downarrow\times2}$ $0.30^{\downarrow\times2}$			$0.30^{\downarrow\times2}$			$0.98^{\downarrow\times2}$	1.96
O3	$0.35^{\downarrow\times2}$	$0.14^{\downarrow\times2}$		$0.53^{\downarrow\times2}$			$0.98^{\downarrow\times2}$		2.00
O4*			$^{2x\rightarrow}0.54^{\downarrow\times2}$		0.37				1.45
O5	0.17		$^{2x\rightarrow}0.42^{\downarrow\times2}$					0.95	1.96
O6	0.04			$^{2x\rightarrow}0.51^{\downarrow\times2}$				0.95	2.01
O7	0.32	0.58				1.08			1.98
O8		$^{2x\rightarrow}0.11^{\downarrow\times2}$			0.49		1.07		1.78
O9	$^{2x\rightarrow}0.03^{\downarrow\times2}$					0.97	0.97		2.00
O10*		0.31		$^{2x\rightarrow}0.51^{\downarrow\times2}$					1.33
Σcations	1.91	2.75	2.70	3.10	2.00	3.95	4.00	3.86	
Theoretical	2.00	3.00	2.64	3.00	2.00	4.00	4.00	4.00	

Notes: left and right superscripts indicate the number of equivalent bonds involving anions and cations, respectively. For sites with mixed occupancy, the bond valences have been weighted according to site populations given in Table 5.

*Anion positions involved in the hydrogen bond O10–H···O4 [*d* (O10···O4) = 2.843(4) Å]. According to Ferraris and Ivaldi (1988), the bond-valence sum (BVS) of such a bond is 0.17 vu. Consequently, the corrected BVS at O4 and O10 sites are 1.62 and 1.16 vu, respectively.

Table 7. Powder X-ray diffraction data (d in Å) for ferriandrosite-(Ce).

I_{obs}	d_{obs}	I_{calc}	d_{calc}	$h\ k\ l$
w	9.3	25	9.21	0 0 1
w	8.2	21	8.12	1 0 0
m	7.8	21	7.82	$\bar{1}$ 0 1
vw	5.17	19	5.16	1 0 1
vw	4.92	7	4.93	$\bar{1}$ 0 2
w	4.69	19	4.683	1 1 0
vw	4.62	10	4.604	0 0 2
vw	3.935	2	3.911	$\bar{2}$ 0 2
w	3.743	11	3.738	$\bar{1}$ 1 2
vw	3.584	11	3.589	0 1 2
ms	3.511	44	3.499	$\bar{2}$ 1 1
w	3.323	14	3.316	2 1 0
vw	3.268	11	3.268	2 0 1
vs	2.895	100	2.888	$\bar{1}$ 1 3
		21	2.887	$\bar{3}$ 0 2
		41	2.865	0 2 0
		14	2.839	2 1 1
m	2.704	11	2.708	3 0 0
		32	2.706	0 1 3
		34	2.702	1 2 0
s	2.615	54	2.610	$\bar{3}$ 1 1
		26	2.580	2 0 2
vw	2.486	5	2.489	$\bar{1}$ 0 4
vw	2.381	11	2.373	$\bar{3}$ 1 3
w	2.316	13	2.311	$\bar{2}$ 2 2
vw	2.261	4	2.265	$\bar{2}$ 1 4
m	2.177	22	2.172	$\bar{4}$ 0 1
		18	2.155	2 2 1
mw	2.112	19	2.109	$\bar{2}$ 2 3
		14	2.095	0 2 3
w	2.032	2	2.034	$\bar{3}$ 2 2
		3	2.031	$\bar{4}$ 1 1
vw	1.963	2	1.958	2 1 3
		2	1.955	$\bar{4}$ 0 4
vw	1.917	16	1.917	2 2 2
w	1.872	10	1.869	$\bar{2}$ 2 4
w	1.829[1]			
w	1.772[1]			
w	1.725[1]			
mw	1.657	13	1.659	$\bar{1}$ 3 3
		10	1.631	$\bar{1}$ 0 6
mw	1.600	21	1.615	$\bar{4}$ 2 4
		12	1.600	$\bar{3}$ 3 1

Notes: Intensity and d_{hkl} were calculated using the software *PowderCell* 2.3 (Kraus and Nolze, 1996) on the basis of the structural model given in Table 3. Only the reflections with I_{calc} > 10 are given, if not observed. Intensities were visually estimated: vs = strong; s = strong; ms = medium–strong; m = medium; mw = medium–weak; w = weak; vw = very weak.
1These reflections correspond to more than two calculated reflections with I < 10.

vanadoandrosite(Ce) and ferriandrosite-(La), respectively (Bonazzi *et al.*, 1996; Cenki-Tok *et al.*, 2006; Nagashima *et al.*, 2015). As discussed by Cenki-Tok *et al.* (2006), the occurrence of Mn^{3+} at the *M*1 site increases the difference between the distances *M*1–O1 and *M*1–O4, owing to the Jahn–Teller effect shown by this cation; this difference is 0.231 and 0.227 Å in manganiandrosite-(La) and manganiandrosite-(Ce), respectively (Bonazzi *et al.*, 1996; Cenki-Tok *et al.*, 2006), whereas in vanadoandrosite-(Ce) and ferriandrosite-(La) this difference is smaller, i.e. 0.161 and 0.137 Å, respectively (Cenki-Tok *et al.*, 2006; Nagashima *et al.*, 2015). In ferriandrosite-(Ce), a difference of 0.145 Å was observed, in agreement with the absence of Mn^{3+} at the *M*1 site.

Three independent Si-centred tetrahedra occur in ferriandrosite-(Ce). Si1 and Si2 are bonded, sharing the O9 atom and forming Si_2O_7 groups; as discussed above, the Si1–O9–Si2 bond angle is sensitive to the occupancy at the *A*1 and the bond length at the *M*3 site. Si3 forms an isolated SiO_4 group. Average bond distances range between 1.624 and 1.637 Å, with bond-valence sums between 3.86 and 4.00 valence units (vu).

Anion sites

Ten independent anion sites occur in ferriandrosite-(Ce). Among them, eight are four-fold coordinated, with bond-valence sums ranging between 1.78 and 2.01 vu; these sites are occupied by $O^{2–}$. Two sites, namely O4 and O10, are three-fold coordinated and are underbonded, with bond-valence sums of 1.45 and 1.33 vu, respectively. The crystal-structure refinement allowed us to locate a residual maximum that was interpreted as a H atom located at 0.95(9) Å from O10. Moreover, the O10···O4 distance, 2.841(4) Å, agrees with a H bond, corresponding to a bond strength, calculated according to Ferraris and Ivaldi (1988), of 0.17 vu. In this way, the correct bond-valence sums at O4 and O10 are 1.62 and 1.16 vu, respectively. These values agree with the mixed nature (O,F) of the O4 site, with an O/(O+F) atomic ratio close to 0.65 (in accord with both chemical and structural data) and the occurrence of (OH) at O10. Moreover, it is worth noting that the O10···O4 is similar to those observed in manganiandrosite-(Ce), ferriandrosite-(La), and vanadoandrosite-(Ce) (ca. 2.87 Å – Cenki-Tok *et al.*, 2006; Nagashima *et al.*, 2015), and shorter than that reported by Bonazzi *et al.* (1996) in manganiandrosite-(La), i.e. 2.94 Å. This difference may be explained considering that the O4 site is bonded to two *M*1 and one *M*3 sites; in all the known species belonging to the androsite series but manganiandrosite-(La), the *M*3 site has a virtually pure M^{2+} occupancy. On the contrary, the latter species has 0.28 M^{3+} apfu, and consequently the bond strength on O4 is higher than in the other cases, thus favouring an elongation (= a weakening) of the H bond.

Relations with other epidote supergroup minerals

Ferriandrosite-(Ce) is a new member of the allanite group, composed, after the addition of this new species, of 18 minerals (Table 8). Five root-names, based on different combinations of cations at the *A*1 and *M*3 sites, are currently known: allanite ($A1 = Ca^{2+}$, $M3 = Fe^{2+}$), akasakaite ($A1 = Ca^{2+}$, $M3 = Mn^{2+}$), androsite ($A1 = Mn^{2+}$, $M3 = Mn^{2+}$), dissakisite ($A1 = Ca^{2+}$, $M3 = Mg^{2+}$), and uedaite ($A1 = Mn^{2+}$, $M3 = Fe^{2+}$).

The name ‘androsite’ was first introduced by Bonazzi *et al.* (1996) on the basis of a sample from a small metamorphic Mn ore body in the Andros Island, Cyclades, Greece. The new species was named ‘androsite-(La)’, later renamed manganiandrosite-(La) by Armbruster *et al.* (2006), owing to the dominance of Mn^{3+} at the *M*1 site. Later, Cenki-Tok *et al.* (2006) described the Ce-analogue manganiandrosite-(Ce) from the Praborna mine (Aosta Valley, Italy), along with the new species vanadoandrosite-(Ce), that has V^{3+} as the dominant cation at the *M*1 position, from a Mn ore deposit located near Vielle-Aure, Hautes-Pyrénées, France. Finally, Nagashima *et al.* (2015) identified the Fe^{3+}-analogue of manganiandrosite-(La), i.e. ferriandrosite-(La) from a Mn deposit in the Mie Prefecture, Japan. The Ce-analogue of this latter species, ferriandrosite-(Ce), is now added to this series. As reported in the Introduction, samples corresponding to this species were reported by Girtler *et al.* (2013) and Kolitsch *et al.* (2021). In particular, the former authors

Table 8. Valid mineral species belonging to the allanite group.

Species	A1	A2	M1	M2	M3	Reference
Allanite-(Ce)	Ca	Ce	Al	Al	Fe^{2+}	Thomson (1811)
Allanite-(La)	Ca	La	Al	Al	Fe^{2+}	Orlandi and Pasero (2006)
Allanite-(Nd)	Ca	Nd	Al	Al	Fe^{2+}	Škoda *et al.* (2012)
Allanite-(Y)	Ca	Y	Al	Al	Fe^{2+}	Nel *et al.* (1949)
Dissakisite-(Ce)	Ca	Ce	Al	Al	Mg	Grew *et al.* (1991)
Dissakisite-(La)	Ca	La	Al	Al	Mg	Tumiati *et al.* (2005)
Ferriakasakaite-(Ce)	Ca	Ce	Fe^{3+}	Al	Mn^{2+}	Biagioni *et al.* (2019)
Ferriakasakaite-(La)	Ca	La	Fe^{3+}	Al	Mn^{2+}	Nagashima *et al.* (2015)
Ferriallanite-(Ce)	Ca	Ce	Fe^{3+}	Al	Fe^{2+}	Kartashov *et al.* (2002)
Ferriallanite-(La)	Ca	La	Fe^{3+}	Al	Fe^{2+}	Kolitsch *et al.* (2012)
Ferriandrosite-(Ce)	Mn^{2+}	Ce	Fe^{3+}	Al	Mn^{2+}	This work
Ferriandrosite-(La)	Mn^{2+}	La	Fe^{3+}	Al	Mn^{2+}	Nagashima *et al.* (2015)
Manganiakasakaite-(La)	Ca	La	Mn^{3+}	Al	Mn^{2+}	Biagioni *et al.* (2019)
Manganiandrosite-(Ce)	Mn^{2+}	Ce	Mn^{3+}	Al	Mn^{2+}	Cenki-Toc *et al.* (2006)
Manganiandrosite-(La)	Mn^{2+}	La	Mn^{3+}	Al	Mn^{2+}	Bonazzi *et al.* (1996)
Uedaite-(Ce)	Mn^{2+}	Ce	Al	Al	Fe^{2+}	Miyawaki *et al.* (2008)
Vanadoallanite-(La)	Ca	La	V^{3+}	Al	Fe^{2+}	Nagashima *et al.* (2013)
Vanadoandrosite-(Ce)	Mn^{2+}	Ce	V^{3+}	Al	Mn^{2+}	Cenki-Toc *et al.* (2006)

first used the name 'ferriandrosite-(Ce)' without approval by the IMA-CNMNC.

The partial replacement of Mn^{2+} by Ca^{2+} at the *A*1 site in androsite-series minerals is in keeping with the possible solid solution between members of this series and those of the akasakaite series, as suggested, for instance, by Biagioni *et al.* (2019), who described strongly zoned grains containing ferriakasakaite-(Ce), manganiandrosite-(Ce), and the potential 'androsite-(Ce)' end-member in samples from the Mn mineralisation of Monte Maniglia, Piedmont, Italy.

As shown in Fig. 4, the occurrence of the 'dollaseite-type' substitution is effective in the androsite series, as previously reported by Cenki-Tok *et al.* (2006). This lead to the appearance of a species having end-member composition $MnCeMgAlMn^{2+}(Si_2O_7)(SiO_4)F(OH)$. Such a composition would correspond to the Mn-analogue of khristovite-(Ce), a species defined by Pautov *et al.* (1993) as $MnCeMgAlMn^{2+}(Si_2O_7)(SiO_4)F(OH)$ and recently described by Ragu *et al.* (2023) as a new mineral, vielleaureite-(Ce). Actually, as discussed by Cenki-Tok *et al.* (2006), there are some doubts about the actual definition of khristovite-(Ce) as the structural data, reported by Sokolova *et al.* (1991), suggests the dominance of Mn^{2+} at the *A*1 site.

Conclusions

Ferriandrosite-(Ce), $Mn^{2+}CeFe^{3+}AlMn^{2+}(Si_2O_7)(SiO_4)O(OH)$, is a new member of the epidote supergroup and another REE-bearing epidote first identified from Mn ore deposits. In this kind of occurrence, epidote-supergroup minerals can host REE and variable amounts of Fe and Mn, showing different oxidation states reflecting the f_{O_2} conditions occurring during the geological evolution of the Mn-rich assemblages.

The possibility of extracting high-quality crystal-chemical information from micrometre-sized volumes of matter, as exemplified by the results obtained on the strongly zoned grains of ferriandrosite-(Ce), opens interesting future scenarios for unravelling the evolution of Mn ore deposits and the ability to shed further light on the complex geological processes shaping our planet.

Acknowledgements. The helpful comments of Principal Editor Stuart Mills and Structural Editor Peter Leverett, as well as two other anonymous reviewers are greatly appreciated. The study was financially supported by VEGA project 2/0029/23 and by Slovak Research and Development Agency project APVV-22-0041. CB acknowledges funding by the Italian Ministero dell'Istruzione, dell'Università e della Ricerca through the project PRIN 2020 "HYDROX – HYDRous-vs-Oxo-components in minerals: adding new pieces to the Earth's H_2O cycle puzzle", prot. 2020WYL4NY.

Supplementary material. The supplementary material for this article can be found at https://doi.org/10.1180/mgm.2023.62.

Competing interests. The authors declare none.

References

Armbruster T., Bonazzi P., Akasaka M., Bermanec V., Chopin C., Gieré R., Heuss-Assbichler S., Liebscher A., Menchetti S., Pan Y. and Pasero M. (2006) Recommended nomenclature of epidote-group minerals. *European Journal of Mineralogy*, **18**, 551–567.

Bajaník Š., Ivanička J., Mello J., Pristaš J., Reichwalder P., Snopko L., Vozár J. and Vozárová A. (1983) *Geological map of the Slovenské Rudohorie Mts. – eastern part 1: 50.000*. Dionýz Štúr Institute of Geology, Bratislava.

Bayliss P. and Levinson A.A. (1988) A system of nomenclature for rare-earth mineral species: revision and extension. *American Mineralogist*, **73**, 422–423.

Biagioni C., Bonazzi P., Pasero M., Zaccarini F., Balestra C., Bracco R. and Ciriotti M.E. (2019) Manganiakasakaite-(La) and ferriakasakaite-(Ce), two new epidote supergroup minerals from Piedmont, Italy. *Minerals*, **9**, 353.

Bonazzi P., Menchetti S. and Reinecke T. (1996) Solid solution between piemontite and androsite-(La), a new mineral of the epidote group from Andros Island, Greece. *American Mineralogist*, **81**, 735–742.

Bosi F., Biagioni C. and Oberti R. (2019a) On the chemical identification and classification of minerals. *Minerals*, **9**, 591.

Bosi F., Hatert F., Hålenius U., Pasero M., Miyawaki R. and Mills S. (2019b) On the application of the IMA-CNMNC dominant-valency rule to complex mineral compositions. *Mineralogical Magazine*, **83**, 627–632.

Brese N.E. and O'Keeffe M. (1991) Bond-valence parameters for solids. *Acta Crystallographica*, **B47**, 192–197.

Bruker AXS Inc. (2022) *APEX 4*. Bruker Advanced X-ray Solutions, Madison, Wisconsin, USA.

Cenki-Tok B., Ragu A., Armbruster T., Chopin C. and Medenbach O. (2006) New Mn- and rare-earth-rich epidote group minerals in metacherts: manganiandrosite-(Ce) and vanadoandrosite-(Ce). *European Journal of Mineralogy*, **18**, 569–582.

Dollase W.A. (1968) Refinement and comparison of the structure of zoisite and clinozoisite. *American Mineralogist*, **53**, 1882–1888.

Faryad S.W. (1994) Mineralogy of Mn-rich rocks from greenschist facies sequences of the Gemericum, West Carpathians, Slovakia. *Neues Jahrbuch für Mineralogie, Monatshefte*, **10**, 464–480.

Ferraris G. and Ivaldi G. (1988) Bond valence vs bond length in O···O hydrogen bonds. *Acta Crystallographica*, B44, 341–344.

Girtler D., Tropper P. and Hauzenberger C. (2013) Androsite-(Ce) and ferriandrosite-(Ce) as indicator for low-grade REE mobility in the Veitsch Mn Deposit (Styria). *Mitteilungen der Österreichischen Mineralogischen Gesellschaft*, **159**, 56.

Grecula P., Abonyi A., Abonyiová M., Antaš J., Bartalský B., Bartalský J., Dianiška I., Ďuďa R., Gargulák M., Gazdačko Ľ., Hudáček J., Kobulský J., Lörincz L., Macko J., Návesňák D., Németh Z., Novotný L., Radvanec M., Rojkovič I., Rozložník L., Varček C. and Zlocha Z. (1995) *Mineral Deposits of the Slovak Ore Mountains, Vol 1*. Geocomplex, Bratislava, 834 pp.

Grew E.S., Essene E.J., Peacor D.R., Su S-C. and Asami M. (1991) Dissakisite-(Ce), a new member of the epidote group and the Mg analogue of allanite-(Ce) from Antarctica. *American Mineralogist*, **76**, 1990–1997.

Holland T.J.B. and Redfern S.A.T. (1997) Unit cell refinement from powder diffraction data: the use of regression diagnostics. *Mineralogical Magazine*, **61**, 65–77.
Kantor J. (1954) On the genesis of manganese ores in the Spišsko-gemerské rudohorie Mts. *Geologické Práce, Zprávy*, **1**, 70–71 [in Slovak].
Kartashov P.M., Ferraris G., Ivaldi G., Sokolova E. and McCammon C.A. (2002) Ferriallanite-(Ce), $CaCeFe^{3+}AlFe^{2+}(SiO_4)(Si_2O_7)O(OH)$, a new member of the epidote group: description, X-ray and Mössbauer study. *The Canadian Mineralogist*, **40**, 1641–1648.
Kolitsch U., Mills S.K., Miyawaki R. and Blass G. (2012) Ferriallanite-(La), a new member of the epidote supergroup from the Eifel, Germany. *European Journal of Mineralogy*, **24**, 741–747.
Kolitsch U., Schachinger T. and Auer C. (2021) Erste mineralogische Untersuchungen an den metamorphen mesozoischen Manganvorkommen der Brandlscharte südlich des Imbachhorns, Kapruner und Fuscher Tal, Salzburg: Nachweise von Alabandin, Cobaltit, Fluorit, Gersdorffit, Gold, Hübnerit, Molybdänit, Percleveit-(La)(?), Sonolith, Thorit, Tsumoit, Ullmannit, Uraninit, Vittinkiit, Zinkgruvanit und weiteren Mineralien. Pp. 209–220 in *Neue Mineralfunde aus Österreich LXX* (Walter, F. *et al.*, editor). Carinthia II, 211/131.
Kraus W. and Nolze G. (1996) POWDER CELL – a program for the representation and manipulation of crystal structures and calculation of the resulting X-ray powder patterns. *Journal of Applied Crystallography*, **29**, 301–303.
Maderspach L. (1875) Die Manganerze von Csucsom und Betlér bei Rosenau im Gömörer Comitate. *Österreichische Zeitschrift für Berg- und Hüttenwesen*, **23**, 548–550.
Mandarino J.A. (1979) The Gladstone-Dale relationship. Part III. Some general applications. *The Canadian Mineralogist*, **17**, 71–76.
Mandarino J.A. (1981) The Gladstone-Dale relationship. Part IV. The compatibility concept and its application. *The Canadian Mineralogist*, **19**, 441–450.
Miyawaki R., Yokoyama K., Matsubara S., Tsutsumi Y. and Goto A. (2008) Uedaite-(Ce), a new member of the epidote group with Mn at the A site, from Shodoshima, Kagawa Prefecture, Japan. *European Journal of Mineralogy*, **20**, 261–269.
Nagashima M., Armbruster T., Akasaka M. and Minakawa T. (2010) Crystal chemistry of Mn^{2+}-, Sr-rich and REE-bearing piemontite from the Kamisugai mine in the Sambagawa metamorphic belt, Shikoku, Japan. *Journal of Mineralogical and Petrological Sciences*, **105**, 142–150.
Nagashima M., Nishio-Hamane D., Tomita N., Minakawa T. and Inaba S. (2013) Vanadoallanite-(La): a new epidote-supergroup mineral from Ise, Mie Prefecture, Japan. *Mineralogical Magazine*, **77**, 2739–2752.
Nagashima M., Nishio-Hamane D., Tomita N., Minakawa T. and Inaba S. (2015) Ferriakasakaite-(La) and ferriandrosite-(La): new epidote-supergroup minerals from Ise, Mie Prefecture, Japan. *Mineralogical Magazine*, **79**, 735–753.
Nel H.J., Strauss C.A. and Wickman F.E. (1949) Lombaardite, a new mineral from the Zaaiplaats Tin Mine, Central Transvaal. *Union of South Africa Department of Mines, Geological Survey Memoir*, **43**, 45–57.
Orlandi P. and Pasero M. (2006) Allanite-(La) from Buca della Vena mine, Apuan Alps, Italy, an epidote group mineral. *The Canadian Mineralogist*, **44**, 63–68.
Pautov L.A., Khorov P.V., Ignatenko K.I., Sokolova E.V. and Nadezhina T.N. (1993) Khristovite-(Ce), (Ca,REE)REE(Mg,Fe) $AlMnSi_3O_{11}(OH)(F,O)$ – a new mineral of the epidote group. *Zapiski Vserossijskogo Mineralogicheskogo Obshchestva*, **122**, 103–111.
Peterec D. and Ďuďa R. (2003) Rare minerals of Mn deposit near Čučma. *Natura Carpathica*, **44**, 229–233 [in Slovak].
Ragu A., Bindi L., Bonazzi P. and Chopin C. (2023) Vielleaureite-(Ce), IMA 2022-134. CNMNC Newsletter 72. *Mineralogical Magazine*, **87**, https://doi.org/10.1180/mgm.2023.21
Rojkovič I. (2001) Early Paleozoic Manganese ores in the Gemericum Superunit, Western Carpathians, Slovakia. *Geolines*, **13**, 34–41.
Shannon R.D. (1976) Revised effective ionic radii and systematic studies of interatomic distances in halides and chalcogenides. *Acta Crystallographica*, A32, 751–767.
Sheldrick G.M. (2015) Crystal structure refinement with SHELXL. *Acta Crystallographica*, **C71**, 3–8.
Škoda R., Cempírek J., Filip J., Novák M., Veselovský F. and Čtvrtlík R. (2012) Allanite-(Nd), $CaNdAl_2Fe^{2+}(SiO_4)(Si_2O_7)O(OH)$, a new mineral from Åskagen, Sweden. *American Mineralogist*, **97**, 983–988.
Sokolova E.V., Nadezhina T.N. and Pautov L.A. (1991) Crystal structure of a new natural silicate of manganese from the epidote group. *Soviet Physics Crystallography*, **36**, 172–174.
Števko, M., Myšľan, P., Biagioni, C., Mauro, D. and Mikuš, T. (2023) Ferriandrosite-(Ce), IMA 2023-022. CNMNC Newsletter 74. *Mineralogical Magazine*, **87**, https://doi.org/10.1180/mgm.2023.54
Thomson T. (1811) Experiments on allanite, a new mineral from Greenland. *A Journal of Natural Phylosophy, Chemistry, and the Arts*, **29**, 47–59.
Tumiati S., Godard G., Martin S., Nimis P., Mair V. and Boyer B. (2005) Dissakisite-(La) from the Ulten zone peridotite (Italian Eastern Alps): a new end-member of the epidote group. *American Mineralogist*, **90**, 1177–1185.
Wilson A.J.C. (editor) (1992) *International Tables for Crystallography, Volume C: Mathematical, Physical and Chemical Tables*. Kluwer Academic, Dordrecht, The Netherlands.

https://doi.org/10.1180/mgm.2023.62 Published online by Cambridge University Press